J. Biophotonics **7**, No. 7, 525–533 (2014) / **DOI** 10.1002/jbio.201200243

Journal of BIOPHOTONICS

FULL ARTICLE

Optical coherence tomography for advanced screening in the primary care office

Ryan L. Shelton[1], *Woonggyu Jung*[1,2], *Samir I. Sayegh*[3], *Daniel T. McCormick*[4], *Jeehyun Kim*[5], *and Stephen A. Boppart*[*,1,6]

[1] Beckman Institute for Advanced Science and Technology, University of Illinois at Urbana-Champaign, Urbana, IL, USA
[2] School of Nano-Bioscience and Chemical Engineering, Ulsan National Institute of Science and Technology, Korea
[3] The Eye Center, Champaign, IL, USA
[4] AdvancedMEMS, San Francisco, CA, USA
[5] Department of Electrical and Computer Engineering, Kyungpook National University, Korea
[6] Departments of Electrical and Computer Engineering, Bioengineering, and Medicine, University of Illinois at Urbana-Champaign, Urbana, IL, USA

Received 24 December 2012, revised 15 March 2013, accepted 16 March 2013
Published online 18 April 2013

Key words: optical coherence tomography, primary care medicine, handheld, portable, screening

Optical coherence tomography (OCT) has long been used as a diagnostic tool in the field of ophthalmology. The ability to observe microstructural changes in the tissues of the eye has proved very effective in diagnosing ocular disease. However, this technology has yet to be introduced into the primary care office, where indications of disease are first encountered. We have developed a portable, handheld imaging probe for use in the primary care setting and evaluated its tissue site accessibility, ability to observe diseased tissue, and screening capabilities in *in vivo* human patients, particularly for pathologies related to the eye, ear and skin. Various stages of diabetic retinopathy were investigated using the handheld probe and early-stage diabetic retinopathy was flagged as abnormal from the OCT images. At such early stages of disease, it is difficult to observe abnormalities with the limited tools that are currently available to primary care physicians. These results indicate that OCT shows promise to transform from being a diagnostic technology in the medical and surgical specialities to a screening technology in the primary care office and at the front-line of healthcare.

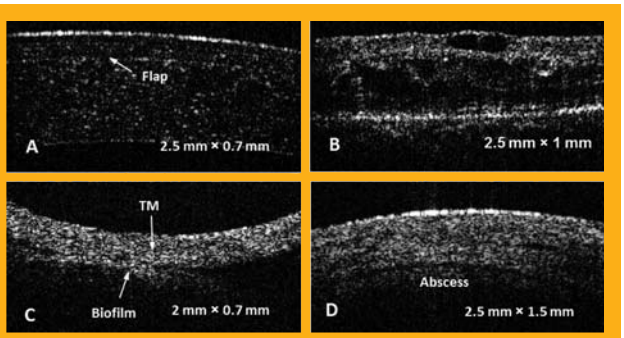

In vivo cross-sectional images of four examples of common pathologies in humans encountered by a primary care physician. All images were taken using a novel handheld OCT imaging probe. (**A**) Human cornea after LASIK surgery. (**B**) Advanced diabetic retinopathy. (**C**) Tympanic membrane with accompanying biofilm. (**D**) Skin abscess showing layer separation and fluid-filled pockets.

* Corresponding author: e-mail: boppart@illinois.edu, Phone: +01 217 333 8598, Fax: +01 217 333 5833

Journal of BIOPHOTONICS

1. Introduction

Primary care physicians, paediatricians, and family practitioners stand at the frontline of the medical field to identify the earliest indications of disease and effectively screen the general population. These medical professionals are required to maintain a broad knowledge of many common diseases and pathologies and typically conduct thousands of patient examinations each year. According to the U.S. Centers for Disease Control and Prevention, 56% of all physician office visits are in the area of primary care, and the average primary care patient visits his/her physician about two times per year [1]. Despite an increasing demand for primary care, especially among the elderly, the percentage of physicians entering the primary care field is declining [2]. Therefore, there is a clear and immediate need for more efficient and effective screening and diagnostic tools in primary care medicine, at the front-line of healthcare.

Despite the obvious important role of primary care physicians, the principal tools used by these physicians have remained largely unchanged for decades. The otoscope and ophthalmoscope, two instruments ubiquitous in primary care, are still essentially instruments used to illuminate and magnify *surfaces* of tissues. These simple tools are coupled with patient histories and information gained from a basic physical exam to make screening and diagnostic decisions that may lead to further imaging and laboratory tests, prescription of treatment medications, or a referral to a specialist.

The otoscope is equipped with a speculum tip and primarily used to visualize the surface of the tympanic membrane (TM) in the ear canal. Coloration and opacity of the TM, along with any visible disruptions in the membrane surface are qualitatively evaluated to determine whether a problem may exist. The otoscope is also suitable to visualize surfaces of the oral mucosa, nasal mucosa, and skin. The ophthalmoscope is mainly used to visualize surface features of the retina. Similar to observations made with an otoscope, coloration, deposits, opacities, and vascular abnormalities in the eye, are qualitatively assessed in order to evaluate ocular or systemic health.

While many serious problems can eventually be detected using these basic tools, there are obvious benefits to realizing effective screening at an earlier disease state. However, during early stages, the hallmarks for disease are more subtle. For this reason, there exists a need to supplement the existing primary care technology with techniques capable of providing more advanced imaging capabilities and real-time *quantitative* feedback, while remaining in a form-factor that is familiar to the physician, user-friendly, and affordable. Technological innovation has revolutionized medicine, and advances in medical imaging are leading examples for screening, detecting, and monitoring disease. While these innovations have advanced the diagnostic power in fields such as radiology and ophthalmology, a similar impact is also possible in primary care medicine.

Optical coherence tomography (OCT) is a relatively new optical imaging technology capable of capturing micron-scale resolution, real-time, 3-D images of biological structures *in vivo* and non-invasively [3]. Analogous to ultrasound imaging, OCT measures the intensity and time-of-flight information collected from backscattered light and uses that information to reconstruct three dimensional reflectivity maps up to several millimetres deep in tissue. These properties, which allow OCT to perform depth-resolved imaging in human tissue while remaining non-invasive and non-ionizing, have led to a wide range of pre-clinical and clinical applications in fields such as ophthalmology [4, 5], cardiology [6, 7], dermatology [8, 9], otolaryngology [10–14], gastroenterology [15, 16], oncology [17–19], and dentistry [20, 21].

While OCT has made a profound clinical impact in the field of ophthalmology in recent years [22–26], its potential has yet to be evaluated for use in primary care medicine, where it may be used as an advanced screening and diagnostic tool across a variety of common tissue sites. Due to its ability to image microstructural changes in tissue morphology, OCT is well-suited for screening in the primary care setting. Many early indicators of common pathology encountered in primary care medicine include morphological changes on the micron-scale. Structural changes such as thickening of the foveal region of the retina, thinning of the retinal nerve fibre layer, and biofilm formation behind the tympanic membrane are all early indications of some of the most common pathologies the primary care physician may encounter when screening the general population. These early indicators are difficult or impossible to observe with conventional primary care optical instruments.

In an effort to address the limitations imposed on the primary care physician by the lack of advanced imaging tools, we have developed a portable OCT system equipped with a novel handheld imaging probe. The probe is integrated into a form factor similar to that of a standard otoscope or ophthalmoscope, providing a familiar platform for the physician and patient. The first generation of this system has been described previously [27]. In this manuscript, we describe several important improvements over the previous design, and investigate the potential for OCT as a screening technology. The improved system was evaluated in several clinical studies and proved successful at identifying early pathological indicators in tissue sites commonly examined in a primary care setting, such as the eye, ear, oral mucosa, and skin.

2. Experimental methods and materials

2.1 Compact OCT system design

The portable imaging system used in this study was designed around a typical fibre-based spectral domain OCT (SD-OCT) configuration, which employed a superluminescent diode (SLD) source (Superlum, Inc.) and a commercial OCT spectrometer (Bayspec, Inc.). The SLD had a spectral bandwidth of 70 nm centred at 830 nm. The spectrometer spatially encoded the wavelengths of the source onto a line scan camera capable of acquiring spectra at a single-line line rate of 70 kHz. All B-mode images in this manuscript were comprised of 1000 A-lines. The light from the SLD was split into sample and reference paths using a 2×2 fibre coupler. The reference path power was controlled with a variable attenuator to prevent saturation of the line scan camera in the spectrometer. Since the portable OCT system is used to image both the anterior segment and the retina of the eye, a flip mirror was placed in the reference arm to allow for a separate, dispersion-compensated path during retinal imaging. Figure 1A shows a schematic of the OCT system along with a 3-D model of the handheld scanner (top right) and a photograph of the portable system (bottom right). The system was packaged inside a medical cart and electrical and fibre connections were routed to the handheld imaging probe through a port in the side of the cart, and encased in plastic tubing for protection.

2.2 Handheld imaging probe design

The sample arm of the OCT system is comprised of a handheld imaging probe which provides the interface through which the physician interacts with the patient. The delivery fibre is terminated by a collimating lens (F220APC-780, Thorlabs) inside the probe enclosure and the light is then directed toward a microelectromechanical systems (MEMS) scanning mirror to provide beam scanning across the tissue. The beam exits the probe head through a port outfitted with a standard otoscope tip. The handheld probe weighs 600 g and the dimensions of the probe enclosure are 10 cm $\times$ 11.25 cm $\times$ 5 cm, with a 12 cm-long ergonomic handle. Figure 1b shows a schematic displaying the anatomy of the handheld imaging probe. A miniature CCD-based colour video camera with a frame rate of 25 Hz and a resolution of 480×640 pixels was integrated into the probe to provide real-time video of the tissue surface under inspection, similar to what the physician would see using a standard otoscope or ophthalmoscope. This video gives the added benefit of visualizing the location of the OCT scanning beam on the tissue. A cold mirror (FMO3, Thorlabs) was used to separate the visible video path from the near-infrared OCT path. While the cold mirror passes most of the reflected OCT illumination, a very small portion does make it onto the camera. This results in the OCT illumination only being visible at the focus, providing the user visual guidance of the location on the tissue where the scan is taking place. The surface of the tissue was illuminated for colour video imaging by a white-light LED and light from this LED was transmitted through delivery fibres terminating at the probe tip.

The metal tip on the probe (see "Metal Probe" in Figure 1B) allows for tissue site-specific attachments to be easily connected and disconnected from the handheld scanner. Figure 2A and B show the handheld probe without a tip, and with an ear speculum tip compatible with standard otoscopes, respec-

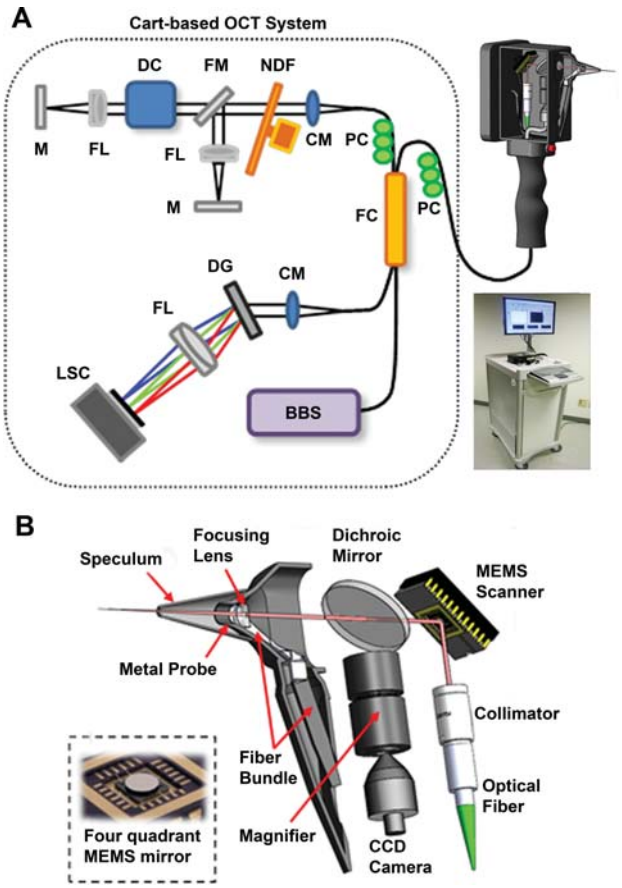

Figure 1 (**A**) Schematic of the portable OCT system and handheld imaging scanner. M: mirror, FL: focusing lens, DC: dispersion compensator, FM: flip mirror, NDF: neutral density filter, CM: collimator, PC: polarization controller, FC: fiber coupler, DG: diffraction grating, LSC: line scanning camera, BBS: broadband source. (**B**) Anatomy of the handheld OCT scanner.

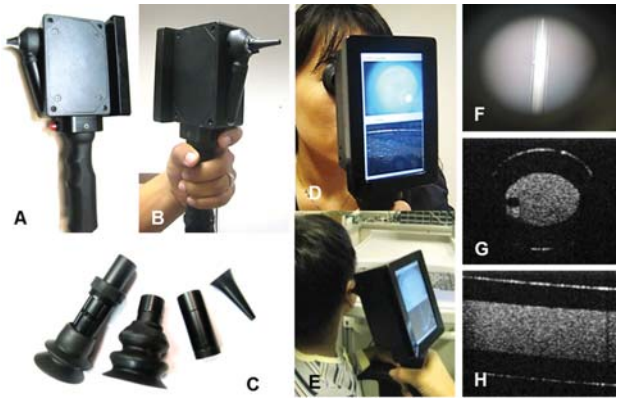

Figure 2 Handheld imaging scanner functionality. (**A**, **B**) Photographs of handheld scanner with and without ear speculum tip, respectively. (**C**) Scanner attachments for retina, anterior segment/skin, oral mucosa, and ear, from left to right in the photo. (**D**, **E**) Photographs of the handheld scanner used for eye (**D**) and ear (**E**) imaging. LCD screen shows color video image and OCT cross-section simultaneously. (**F**–**H**) Example of cross-pattern scanning. A color video image of a capillary tube filled with Intralipid, taken using the scanner, is shown in (**F**). A cross-sectional slice of the tube is shown in (**G**) and a longitudinal slice is shown in (**H**). This demonstrates the usefulness of having an alternating two-axis scan pattern, rather than a single B-scan axis.

tively. Figure 2C shows the available tip attachments for imaging in the retina, anterior segment of the eye, skin and oral mucosa, and the ear. Each attachment screws onto the metal probe tip in the same fashion as an ear speculum. The retinal attachment also includes a focal length adjustment collar in order to compensate for variations in size and shape of refractive elements in the eyes of different patients.

2.3 Improvements over previous designs

Several important and useful improvements were made to the previous handheld probe design. The two most significant of these improvements are an LCD touchscreen located on the back of the handheld probe and the addition of a MEMS scanner in place of the previous galvanometer-scanning implementation. MEMS scanning devices are becoming increasingly more common in OCT systems, particularly handheld units and catheters [28–30], due to their small form factor. The LCD touchscreen (shown in Figure 2D and E) provides a way for the physician to visualize both the video display from the CCD camera (top half of the screen) and the cross-sectional depth image from the OCT system (bottom half of the screen) without having to look away from the patient. The MEMS scanner used in this study utilized a four-quadrant scanning mechanism (shown in the inset of Figure 1B). Unlike single-quadrant MEMS scanners, which can only tilt from 0 degrees to a specified positive angle, four-quadrant scanners can be operated across positive and negative tilt angles along both axes. This functionality typically allows for a larger scanning field-of-view as well as simplified alignment procedures due to the fact that the centre of the scan truly represents 0 degrees. The resonant frequencies of the MEMS scanner were 323 Hz and 330 Hz in the x- and y-axes, respectively, and the maximum tilt angles were greater than 15 degrees along each axis. The dimensions of the MEMS device are 15 mm × 20 mm × 2 mm with a 3.2 mm mirror. It is important to note that this MEMS device is a statically actuated device, which allows it to operate at any speed up to its resonant frequency. This, combined with the fact that the two axes are decoupled, means that fully arbitrary scan patterns and scan rates may be realized. In addition to standard raster scanning, radial scanning has been used successfully with this device, and the capability to perform arbitrary point scans is available.

The MEMS scanner provides several advantages. By using the MEMS scanner, the OCT system speed was limited only by the line rate of the spectrometer. Additionally, the form factor of the MEMS device is significantly smaller than the footprint of the galvanometer scanners previously used. Finally, the MEMS scanner uses a single mirror for dual axis scanning, which allows for truly telecentric light delivery, in contrast to a galvanometer pair, in which each mirror lies in a separate plane along the optical axis.

In an effort to make the handheld probe as user-friendly as possible for physicians, an auditory indicator was also implemented, which alerts the user when the tissue of interest is near the focus of the OCT beam. Any time a reflected OCT signal meets certain threshold criteria, an intermittent tone is heard. The repetition frequency of the tone then increases as the reflected signal moves closer to the optical focus of the OCT scanner. This auditory feedback assists the physician in positioning the beam focus on the tissue site quickly, which can be difficult when imaging sites such as the TM, which lies deep within the ear canal.

Additional improvements over the previous design include an ergonomic handle for ease-of-use and robust probe redesign allowing all fibres and cables to be completely encased in the plastic tubing and probe head enclosure.

Physicians desire real-time feedback of tissue structure. While the computing power of our current system did not allow for the acquisition and rendering of large 3-D volumes under normal real-time operation, an alternative scanning pattern was developed. Typically, a single B-scan image gives only a very limited picture of the structure under investiga-

tion. As a reasonable compromise, we elected to alternate B-scan locations in an X–Y cross pattern. This allows the physician to visualize two orthogonal slices through a given volumetric field-of-view, providing a more informative data set without sacrificing real-time feedback. This functionality is demonstrated in Figure 2F, G, and H. Figure 2F shows a colour video image of a glass capillary tube filled with 10% Intralipid. Figure 2G and H show the transverse and longitudinal cross-sections of the tube, respectively. Observing the signal through both orthogonal planes gives a much better representation of the capillary tube.

2.4 Human subjects

All human subject protocols were approved by the Institutional Review Board at the University of Illinois at Urbana-Champaign. Six human subjects were recruited for this study: one control and five with varying degrees and types of pathology. All patients were imaged with the described portable OCT system and handheld probe. Imaging was performed at The Eye Center in Champaign, IL and the Beckman Institute for Advanced Science and Technology at the University of Illinois at Urbana-Champaign.

3. Results and discussion

3.1 Survey of accessible tissue sites

An array of images was acquired in order to demonstrate the breadth of imaging sites accessible to the handheld OCT probe. Figure 3 shows *in vivo* human tissue imaged in cross-section with the handheld OCT probe. Figure 3A–I shows images of a fingernail plate and fold, skin of the fingertip (sweat duct labelled), oral mucosa along the gum line, tooth with accompanying gum tissue, tympanic membrane in the ear, angle of the eye, cornea, retina, and optic nerve head, respectively. All of these tissue sites are commonly examined by primary care physicians (typically with several different devices) and are part of a general health exam. As can be seen in the images, there are many details and structures of interest at these sites that cannot be observed with only the surface imaging capabilities of a standard otoscope or ophthalmoscope.

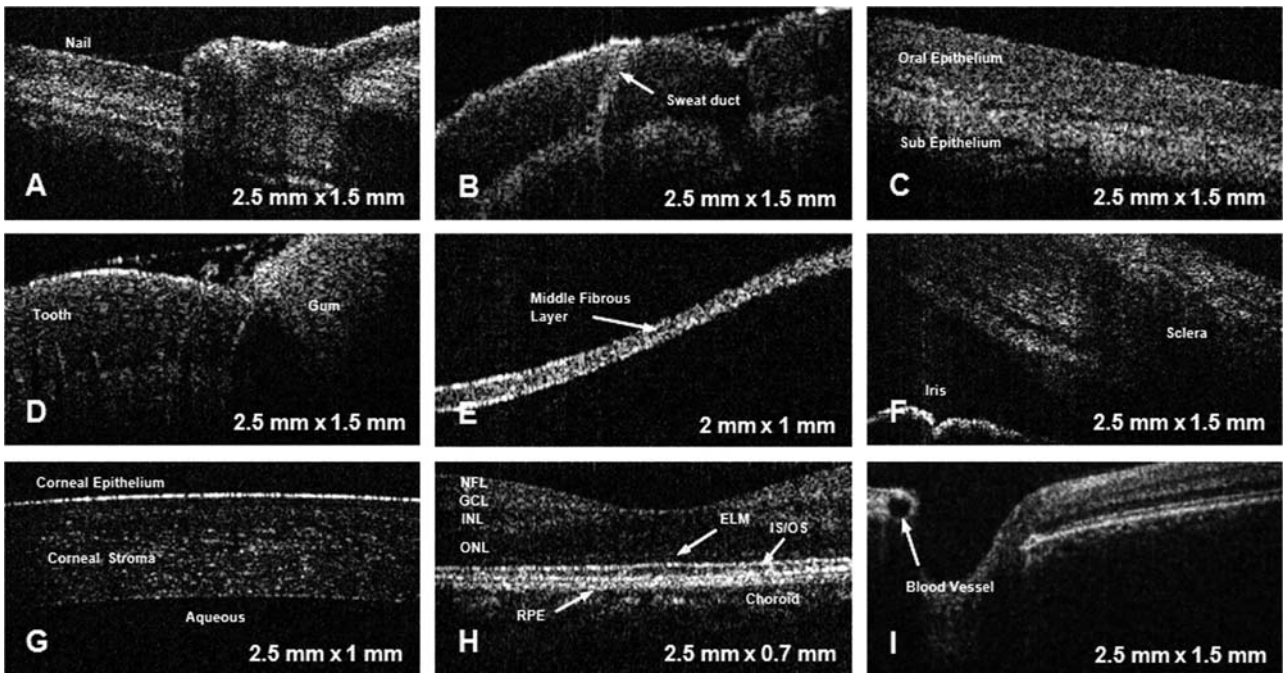

Figure 3 *In vivo* OCT images acquired from normal human tissue. (**A**) fingernail plate and fold, (**B**) skin at the fingertip with accompanying sweat duct, (**C**) oral mucosa along gum line, (**D**) tooth with adjacent gum tissue, (**E**) tympanic membrane in the ear, (**F**) angle of the eye showing iris and sclera, (**G**) cornea, (**H**) fovea of the retina showing retinal layers, (**I**) retina around the optic nerve head. Abbreviations: NFL, nerve fiber layer; GCL, ganglion cell layer; INL, inner nuclear layer; ONL, outer nuclear layer; ELM, external limiting membrane; IS/OS, junction between the inner and outer segment of the photoreceptors; RPE, retinal pigment epithelium.

3.2 Observation and screening for pathologies

In addition to the microstructural details indicated in the previous normal images, many early pathological changes can be observed with OCT. There is a wide array of pathologies that primary care physicians encounter regularly when screening the general population for disease. Figure 4 highlights some of these conditions *in vivo* in human subjects by displaying orthogonal cross-sectional (X–Z and Y–Z) views of the tissue under observation. Figure 4A and B show sagittal and transverse cross-sections of the cornea of a patient after corrective LASIK surgery. The corneal flap which is cut and repositioned during surgery is clearly visualized in these images. Figure 4C and D show coronal and transverse cross-sections of the tympanic membrane of the ear. In this case, the patient had chronic otitis media, which has been linked to the formation of biofilms behind the TM [31, 32]. A clear distinction can be made in the images between the highly scattering, smooth TM and the lower scattering, less organized biofilm. Figure 4E and F show sagittal and transverse cross-sections from an abscess located on the forehead. The OCT images show clear separation of layers in the tissue caused by infection and fluid accumulation, indicated by the signal-poor bands within the image.

One of the chief responsibilities of a primary care physician is to screen patients for disease indicators, and refer them to a medical specialist if an abnormality appears that may be indicative of a more serious pathological problem. In order to evaluate the handheld OCT probe as a screening technology in the primary care office, the retinas of one control patient and three patients with various degrees of diabetic retinopathy were imaged. Figure 5 shows eight OCT retinal images: one normal control image set (A, B), and three image sets depicting varying severity of diabetic retinopathy (C–H). Each image set (row) is a pair consisting of sagittal (left column) and transverse (right column) cross-sections of the central macula, obtained from human patients. The second image set (C, D) shows early stage macular edema, a common manifestation of diabetic retinopathy. The overall thickening of the retina is a common characteristic of this condition. The third image set (E, F) shows a more advanced case of macular edema, in which macular thickness has increased (see arrow). Additionally, fluid has started accumulating throughout the thickness of the retina. The fourth image set (G, H) illustrates a more advanced stage of macular edema with increased thickening and formation of multiple cysts.

Advanced diabetic retinopathy, and in particular, macular edema, can be diagnosed in a primary care clinic with a direct ophthalmoscope due to retinal thickening and retinal deposits. However, in early cases, such as the one depicted in Figure 5C, D, it may be very difficult for a primary care physician using a direct ophthalmoscope to detect or identify pathology. In the unlikely event that the patient is complaining about poor vision at this early stage, the physician may initiate a referral to a specialist. However, significant damage to the retina may be avoided

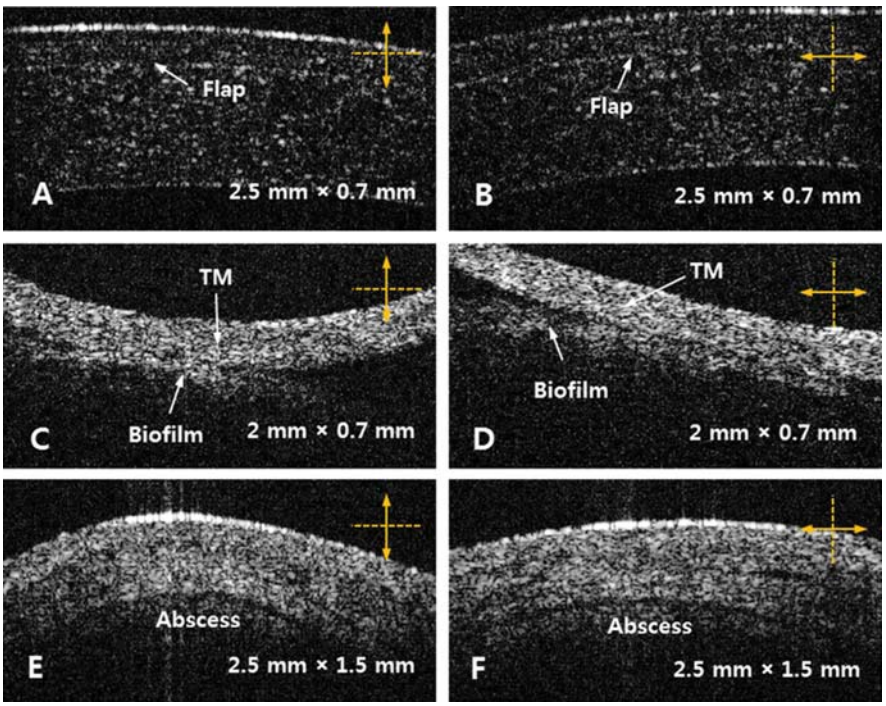

Figure 4 Examples of common pathologies imaged with the OCT handheld scanner. (**A**, **B**) shows the cornea of a patient who has undergone LASIK corrective surgery. (**C**, **D**) shows a tympanic membrane with accompanying bacterial biofilm from a patient with chronic otitis media. (**E**, **F**) shows an abscess from the forehead of a human male. Pockets of fluid and layer separation can be seen as a result of the infection. The double-headed arrows show the direction of the scan that occurred in the X–Y (transverse) plane across the tissue, and each pair of images represents the two orthogonal (X–Z and Y–Z) planes.

if the patient is promptly referred during the earlier stages of diabetic retinopathy. Indeed, the Early Treatment Diabetic Retinopathy Study (ETDRS) has clearly demonstrated the benefits of early intervention [25]. More recent work suggests the relevance of an even earlier intervention based on OCT findings [26] and the availability of additional successful treatment modalities [27].

Due to the breadth of pathologies and tissue sites that primary care physicians must be familiar with, it is helpful, perhaps essential, to simplify the image data as much as possible and provide direct analysis that may help guide screening or making a diagnosis. With this in mind, we are actively pursuing novel methods for segmentation and classification of normal vs. pathological tissue at the tissue sites shown above. The goal is to provide the physician with a single number or binary outcome to supplement their screening, assessment, and diagnosis, rather than requiring them to learn to interpret these images directly.

OCT has been used extensively by ophthalmic specialists for diagnosing and monitoring ocular diseases, including glaucoma, diabetic retinopathy and macular degeneration. However, as the results of this study indicate, OCT may also be valuable as a screening technology. Many pathological processes start beneath the most superficial aspects of the involved organ/tissue. For this reason it is more difficult to detect and identify the earliest stages of these pathologies when observation is restricted to surface observation. If primary care physicians are given more advanced optical imaging tools to observe subsurface structural changes in the tissues they commonly examine, they may be able to detect and diagnose at earlier stages of disease progression, make quantitative rather than qualitative assessments, perform measurements that can be tracked longitudinally over multiple visits, and make more accurate and appropriate referrals to specialists. All of these are likely to result in better outcomes for patients and potentially reduce the cost of quality healthcare.

An important aspect of future adoption of this technology in primary care facilities is cost. Unlike specialists, primary care physicians must evaluate a broad range of tissue sites and pathologies. This makes specialized equipment, such as the desktop OCT systems found in ophthalmologists' offices, unfeasible for a typical primary care facility because of the high cost for a piece of equipment that only addresses a small fraction of patient problems. How-

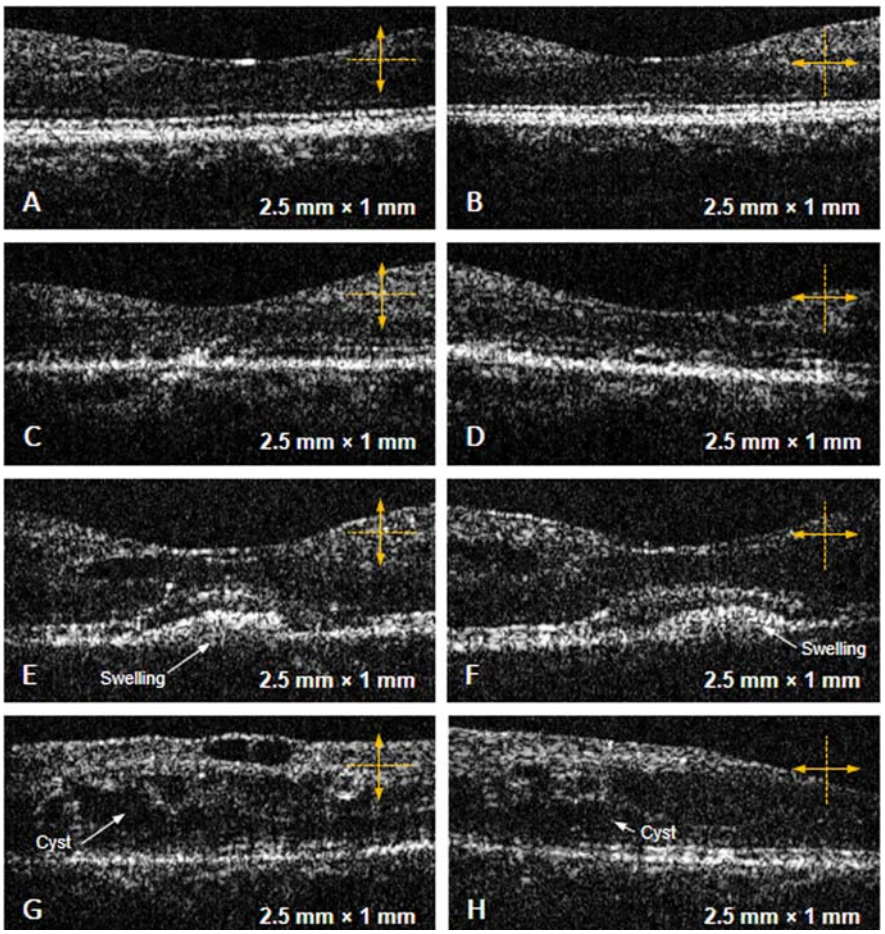

Figure 5 OCT images of the macular region of the retina in patients with various stages of diabetic retinopathy. (**A**, **B**) Normal retina from a control patient. (**C**, **D**) Early-stage diabetic retinopathy, showing disturbance of the layers near the choroid. (**E**, **F**) Diabetic retinopathy with accompanying macular edema. Swelling and thickening of the retina is evident. (**G**, **H**) Advanced diabetic retinopathy. Cysts, or pockets of fluid are found throughout the thickness of the retina. The double-headed arrows show the direction of the scan that occurred in the X–Y (transverse) plane across the tissue, and each pair of images represents the two orthogonal (X–Z and Y–Z) planes.

ever, technology essential to OCT, such as broadband light sources and spectrometers, are drastically dropping in price, paving the way for low-cost OCT systems. It is reasonable to assume that a clinic could invest in one or two portable OCT units to share amongst its physicians, much like EKG machines are currently shared. With this in mind, a price point of less than US $ 10,000 is not unreasonable, assuming the impact on patient outcomes is sufficient. This price point for a basic OCT system is expected to be realized within the next few years.

4. Conclusion

A portable, handheld OCT device has been developed and evaluated in the primary care context. The portable OCT system was integrated with a handheld probe resembling a standard otoscope or ophthalmoscope to provide a familiar platform for the primary care physician. This technology is aimed at transforming OCT from a diagnostic modality to a screening modality for assessing primary care patients with early-stage disease, for making quantitative longitudinal assessments, and ultimately for improving the accuracy with which the physician can make referrals or implement treatment plans in early stages of disease. While OCT has commonly been used by medical and surgical specialists as a diagnostic imaging technology, its merit for disease screening in the primary care context remains to be fully investigated.

In this study, the handheld OCT probe was used to image a variety of *in vivo* human tissue sites that are commonly examined by a primary care physician during a general health examination. Tissue pathologies were investigated, including a cornea after LASIK surgery, an infected middle ear and tympanic membrane with accompanying biofilm, and an infected skin abscess. Finally, OCT was demonstrated as a screening technology in the primary care office by acquiring images of normal retina and varying stages of diabetic retinopathy in human subjects. The handheld OCT probe was capable of detecting structural abnormalities in the retina of a patient with early-stage diabetic retinopathy, before such indications would be observed in the surface images from an ophthalmoscope. These results demonstrate that in addition to its current diagnostic applications, OCT may prove useful as a screening technology.

Acknowledgements We thank Darold Spillman for operational and information technology support for this research, Eric Chaney for assistance with IRB protocols and human subject consenting, and Jessica Taibl for clinical support. This research was completed with the following contributions: R.L.S. assembled and analysed the data, and wrote the paper with assistance from S.I.S. and S.A.B.; W.J. constructed the OCT system and handheld probe and collected data; S.I.S. performed all medical and surgical ophthalmic procedures, contributed design modification to the handheld device that facilitated efficient acquisition, and supervised all clinical aspects related to the collection and analysis of ophthalmic data; D.T.M. designed and fabricated the MEMS scanner and assisted with integration; J.K. assisted with the design of the OCT system; S.A.B. conceived of and managed this research, obtained funding, analysed data, and edited the paper. This research was supported in part by grants from the U.S. National Institutes of Health (NIBIB Bioengineering Research Partnership R01 EB013723, and NIBIB R01 EB012479, S.A.B.), and Sponsored Research Agreements from Welch Allyn, Inc. and Blue Highway, LLC. Additional information can be found at http://biophotonics.illinois.edu and http://2020eyecenter.com.

Author biographies Please see Supporting Information online.

References

[1] Center for Disease Control and Prevention. (2012, 9/15/12). Ambulatory Care Use and Physician Visits. Available: http://www.cdc.gov/nchs/fastats/docvisit.htm
[2] National Institutes of Health. (2008, 9/15/12). *Primary Care Providers – Preliminary Literature Review*. Available: http://www.nei.nih.gov/nehep/research/PrimaryCareProviders.pdf
[3] D. Huang, E. A. Swanson, C. P. Lin, J. S. Schuman, W. G. Stinson, W. Chang, M. R. Hee, T. Flotte, K. Gregory, C. A. Puliafito, and J. G. Fujimoto, Science **254**, 1178–1181 (1991).
[4] B. Cense, N. A. Nassif, T. C. Chen, M. C. Pierce, S. H. Yun, B. H. Park, B. E. Bouma, G. J. Tearney, and J. F. de Boer, Opt. Express **12**, 2435–2447 (2004).
[5] R. A. Costa, M. Skaf, L. A. S. Melo, D. Calucci, J. A. Cardillo, J. C. Castro, D. Huang, and M. Wojtkowski, Prog. Retin. Eye Res. **25**, 325–353 (2006).
[6] V. Y. Lim, L. Buellesfeld, and E. Grube, Heart **92**, 409 (2006).
[7] H. Yabushita, B. E. Bouma, S. L. Houser, H. T. Aretz, I. K. Jang, K. H. Schlendorf, C. R. Kauffman, M. Shishkov, D. H. Kang, E. F. Halpern, and G. J. Tearney, Circulation **106**, 1640–1645 (2002).
[8] J. Welzel, Skin Res. Technol. **7**, 1–9, 2001.
[9] S. Neerken, G. W. Lucassen, M. A. Bisschop, E. Lenderink, and T. A. Nuijs, J. Biomed. Opt. **9** 274–281 (2004).
[10] H. R. Djalilian, M. Rubinstein, E. C. Wu, K. Naemi, S. Zardouz, K. Karimi, and B. J. Wong, Otol. Neurotol. **31**, 932–935 (2010).
[11] H. M. Subhash, A. Nguyen-Huynh, R. K. Wang, S. L. Jacques, N. Choudhury, and A. L. Nuttall, J. Biomed. Opt. **17**, 060505 (2012).
[12] S. S. Gao, A. Xia, T. Yuan, P. D. Raphael, R. L. Shelton, B. E. Applegate, and J. S. Oghalai, Opt. Express **19**, 15415–15428 (2011).

[13] B. J. Wong, R. P. Jackson, S. Guo, J. M. Ridgway, U. Mahmood, J. Su, T. Y. Shibuya, R. L. Crumley, M. Gu, W. B. Armstrong, and Z. Chen, Laryngoscope **115**, 1904–1911 (2005).
[14] C. Pitris, K. T. Saunders, J. G. Fujimoto, and M. E. Brezinski, Arch. Otolaryngol. Head Neck Surg. **127**, 637–642 (2001).
[15] S. Mordon, V. Maunoury, P. Bulois, P. Desreumaux, and J. F. Colombel, Gastroenterol. Clin. Biol. **29**, 618–620 (2005).
[16] J. M. Poneros and N. S. Nishioka, Gastrointest. Endosc. Clin. N. Am. **13**, 309–323 (2003).
[17] W. B. Armstrong, J. M. Ridgway, D. E. Vokes, S. Guo, J. Perez, R. P. Jackson, M. Gu, J. Su, R. L. Crumley, T. Y. Shibuya, U. Mahmood, Z. Chen, and B. J. Wong, Laryngoscope **116**, 1107–1113 (2006).
[18] M. T. Tsai, H. C. Lee, C. K. Lee, C. H. Yu, H. M. Chen, C. P. Chiang, C. C. Chang, Y. M. Wang, and C. C. Yang, Opt. Express **16**, 15847–15862 (2008).
[19] F. T. Nguyen, A. M. Zysk, E. J. Chaney, S. G. Adie, J. G. Kotynek, U. J. Oliphant, F. J. Bellafiore, K. M. Rowland, P. A. Johnson, and S. A. Boppart, IEEE Eng. Med. Biol. Mag. **29**, 63–70 (2010).
[20] L. L. Otis, M. J. Everett, U. S. Sathyam, and B. W. Colston, Jr., J. Am. Den.t Assoc. **131**, 511–514 (2000).
[21] H. Kang, J. J. Jiao, C. Lee, M. H. Le, C. L. Darling, and D. Fried, IEEE J. Sel. Top. Quantum Electron. **16**, 870–876 (2010).
[22] X. Qiu, L. Gong, X. Sun, and H. Jin, Cornea **30**, 543–549 (2011).
[23] M. Pircher, C. K. Hitzenberger, and U. Schmidt-Erfurth, Prog. Retin. Eye Res. **30**, 431–451 (2011).
[24] J. Wang, M. Abou Shousha, V. L. Perez, C. L. Karp, S. H. Yoo, M. Shen, L. Cui, V. Hurmeric, C. Du, D. Zhu, Q. Chen, and M. Li, Ophthal. Surg. Lasers Imag. **42** (Suppl.), S15–S27 (2011).
[25] C. Dai, C. Zhou, S. Fan, Z. Chen, X. Chai, Q. Ren, and S. Jiao, Opt. Express **20**, 6109–6115 (2012).
[26] R. de Kinkelder, D. M. de Bruin, F. D. Verbraak, T. G. van Leeuwen, and D. J. Faber, J. Biophotonics **6,** 314–320 (2013).
[27] W. Jung, J. Kim, M. Jeon, E. J. Chaney, C. N. Stewart, and S. A. Boppart, IEEE Trans. Biomed. Eng. **58**, 741–744 (2011).
[28] J. Sun, S. Guo, L. Wu, L. Liu, S. W. Choe, B. S. Sorg, and H. Xie, Opt. Express **18**, 12065–12075 (2010).
[29] K. H. Kim, J. A. Burns, J. J. Bernstein, G. N. Maguluri, B. H. Park, and J. F. de Boer, Opt. Express **18**, 14644–14653 (2010).
[30] J. C. Yin, G. J. Liu, J. Zhang, L. F. Yu, S. Mahon, D. Mukai, M. Brenner, and Z. P. Chen, J. Biomed. Opt. **14**, 060503 (2009).
[31] L. Hall-Stoodley, F. Z. Hu, A. Gieseke, L. Nistico, D. Nguyen, J. Hayes, M. Forbes, D. P. Greenberg, B. Dice, A. Burrows, P. A. Wackym, P. Stoodley, J. C. Post, G. D. Ehrlich, and J. E. Kerschner, JAMA **296**, 202–211 (2006).
[32] C. T. Nguyen, W. Jung, J. Kim, E. J. Chaney, M. Novak, C. N. Stewart, and S. A. Boppart, Proc. Natl. Acad. Sci. USA **109**, 9529–9534 (2012).